The Egyptian Journal of Radiology and Nuclear Medicine (2016) 47, 275–289

Egyptian Society of Radiology and Nuclear Medicine

The Egyptian Journal of Radiology and Nuclear Medicine

www.elsevier.com/locate/ejrnm
www.sciencedirect.com

ORIGINAL ARTICLE

# The role of MRI and MRS in the diagnosis of non hydrocephalic macrocrania in infancy and early childhood

**Dalia M. Moussa** [a,*], **Abdel Aziz El Nekeidy** [a], **Ahmed M. Abougabal** [a], **Tarek I. Omar** [b], **Tarek R. Saleh** [a]

[a] *Department of Radiodiagnosis, Faculty of Medicine, University of Alexandria, Egypt*
[b] *Department of Pediatrics, Faculty of Medicine, University of Alexandria, Egypt*

Received 26 March 2015; accepted 28 September 2015
Available online 29 October 2015

**KEYWORDS**

MRI;
MRS;
Non hydrocephalic macrocrania;
Dysmyelinating;
Glutaric aciduria

**Abstract** The aim of this study was to determine the key MRI findings in different disease causing macrocrania in early childhood that will help in early detection and diagnosis.

*Patients and methods:* This study was conducted on 20 patients (their age ranged from 3.5 months to 5 years) referred to the radiodiagnosis department in the period between February 2013 and June 2014. All patients were subjected to conventional MRI. MRS was done in 8 cases using PRESS 3D multi-voxel chemical shift imaging.

*Results:* The patients subdivided into 7 groups. Glutaric aciduria type 1 (40%) MRI showed wide operculum sign; MRS done in 4 patients showed elevated choline with preserved NAA peak. Benign macrocrania of infancy (15%), and MRI showed enlarged cranio-cortical and inter-hemispheric subarachnoid spaces beyond 5 mm, mildly dilated ventricles. Van der Knaap disease (15%) showed bilateral symmetrical confluent white matter dysmyelination with bilateral fronto-temporal subcortical cystic changes .MRS done in 2 patients showed increase in Cho/NAA ratios. Mucopolysaccharidosis (10%) showed dilated Virchow Robin spaces. MRS done in one patient showed decreased NAA, and increased choline/creatine ratio. Canavan disease (10%) MRI showed bilateral symmetrical extensive white matter dysmyelination. MRS showed markedly elevated NAA. Alexander disease (5%) showed bilateral symmetrical white matter dysmyelination with frontal predilection. MRS revealed increased NAA/Cr, increased myo-inositol/Cr, and lactate doublet. Gangliosidosis (5%) MRI showed bilateral symmetrical T2 and FLAIR hyperintense putamen. CT showed bilateral symmetric thalamic hyperdensities.

*Conclusion:* MRI can diagnose different causes of non hydrocephalic macrocrania. MRS is helpful in differentiating benign macrocrania of infancy from dysmyelinating diseases and is specific in Canavan Disease.



* Corresponding author.

Peer review under responsibility of Egyptian Society of Radiology and Nuclear Medicine.

http://dx.doi.org/10.1016/j.ejrnm.2015.09.009

## 1. Introduction

Macrocrania is a common pediatric clinical condition affecting up to 5% of the population (1). Head circumference measurement is an important physical examination to evaluate childhood growth and development because deviations from normal head growth patterns can indicate an underlying congenital, genetic, or acquired neurologic problem (2). Macrocephaly is defined as an occipitofrontal circumference (OFC) of two standard deviations (SD) or more above the mean for age, gender, and gestation ($\geqslant$97th percentile) (1). Magnetic resonance (MR) imaging of the infant brain has given an enormous insight into the maturational processes that take place after birth that is not possible with computed tomography or ultrasound (3).

Common causes of macrocephaly (MC) include familial megalencephaly (larger-than-normal brain mass), benign extra-cerebral collections of infancy (BECC) and hydrocephalus (HC). Macrocephaly without HC may also be seen in some genetic, metabolic, and dysplastic syndromes or may be caused by tumors and cysts, pseudotumor cerebri, or subdural collections (e.g., hematomas, hygromas) (4).

Macrocrania is most commonly a result of familial macrocrania and represents a normal variation in head size but may also be a sign of an underlying abnormality requiring further investigation. The keys in making this distinction are the trend in head circumference growth and physical examination. In familial macrocrania, the head circumference may spike at 4–6 months of age above the ninety-eight percentile but then maintains its curve on the head circumference growth chart over time. Pathologic macrocephaly continues to increase (5).

Idiopathic external hydrocephalus is a benign self-limiting condition that usually resolves without treatment (6).

In the pediatric population, chronic subdural fluid collection is group of related condition termed as extracerebral (or extra-axial) fluid collection (7). Chronic subdural fluid collection can present as chronic subdural hematoma or subdural effusion (7).

Modern neuroimaging techniques are used to distinguish external hydrocephalus from a subdural fluid collection (e.g., chronic subdural hematoma) (6).

Megalencephaly is as a rule accompanied by macrocephaly. Megalencephaly is divided into an anatomic type (developmental) and a metabolic type. Metabolic megalencephaly refers to various storage and degenerative encephalopathies (8).

The differential diagnosis includes Alexander's disease, Canavan's disease, glutaric aciduria type 1, GM1 and GM2 gangliosidosis, merosin-deficient variant of congenital muscular dystrophy and megalencephalic leukoencephalopathy with subcortical cysts (MLC) (8).

Examples of metabolic disorders are the mucopolysaccharidosis (MPS), GM2-gangliosidoses, and glutaric aciduria type I (9).

The aim of this study was to determine the key MRI findings in different disease causing macrocrania in infancy and early childhood that will help in early detection and diagnosis.

## 2. Material and methods

This study was conducted on 20 patients who are having macrocrania and have been referred to the department of radiodiagnosis in a period from 1/2/2013 till 31/6/2014.

Inclusion criteria were patient age from 3.5 month up to 5 years of age and head circumference: greater than 98th percentile.

Exclusion criteria were children with macrocrania having hydrocephalus and children with macrocrania secondary to neoplasm.

The study has been approved by the formal ethical committee.

An informed consent from the patient parents or caregivers was taken.

Conventional MRI and MR spectroscopy examinations were performed in a single session on a 1.5-T multi-voxel MR unit (Signa Horizon 1.5; GE Medical Systems, Milwaukee, WI).

The examination included at least the following three sequences: T1 weighted images [echo time (TE)/repetition time (TR) 11 ms/550 ms], T2-fast spin echo (FSE) sequence in axial plane (TR/TE = 4000/120 ms) and T2-Fluid-attenuated inversion-recovery (FLAIR) sequence in axial plane (TR/TE = 7000/128 ms, TI = 1750 ms). For these sequences slice thickness = 5 mm, gap = 1 mm, acquisition matrix = 256 × 256, FOV = 240 mm. In some patients, the following sequences were done: T1 postcontrast axial sequence (only if there was anterior white matter predilection like in Alexander disease). T1 3D spoiled gradient echo sequence *(SPGE)* (TR)/TE) = 12.67/5.35 ms, slice thickness = 1.4 mm, acquisition matrix = 256 × 256, Field of view (FOV) = 240 mm, Inversion time (TI) = 400 ms). Diffusion weighted imaging: Transverse single-shot echo-planar diffusion-weighted imaging (TR/TE: 5200/105 ms; section thickness: 5 mm; intersection gap: 1 mm; acquisition matrix: 128 × 128; FOV: 240 mm; b value: 1000) which was not available in all patients as it was a retrospective study.

Magnetic Resonance Spectroscopic (MRS) Imaging was done in 8 patients: MR spectra were obtained by using phase encoded point-resolved spectroscopy sequence (PRESS) 3D multi-voxel chemical shift imaging (CSI) with the following parameters; 15-mm section thickness, spin-echo sequence (2000/144/1) with outer volume suppression. The field of view was 24 cm, with 32 × 32 phase-encoding steps, rendering a nominal voxel size of 0.8 $cm^3$. Water suppression was accomplished with a single chemical shift selective pulse with a bandwidth of 110 Hz. Extracranial lipid signals were attenuated by the use of six outer volume saturation pulses.

Three main sites were examined by MRS at which a volume of interest was positioned on the axial MRI images: 1. basal ganglia/deep gray matter nuclei, 2. corona radiata and centrum semiovale being the most common examined sites in case of normal appearing white matter, and 3. ventricular CSF. The full time of examination (including conventional MRI with the abovementioned protocol, DWI and MRS) was in the range of 20–25 min for each patient.

## 3. Results

This study included 20 cases who are having macrocrania and have been referred to the department of radiodiagnosis in a period from 1/2/2013 till 31/6/2014 (see Diagram 1).

The study was mixed prospective (12 patients) and retrospective study depending on the available patients' medical records from the neurology clinic in el shatby hospital.

The age of the twenty patients ranged between 3.5 months and 5 years (mean age = 21 month).

Eight patients (40%) were males and twelve patients (60%) were females. The patients had various clinical manifestations in addition to macrocephaly (100%), 11 patients showed delayed milestones (55%), 7 patients complained of seizures (35%), 5 had psychomotor regression (25%), and 2 patients complained of hypotonia (10%).

For better description of the MRI features, we have subdivided the 20 patients into 7 groups according to the cause of macrocrania by the consensus of the available clinical, laboratory, radiological and genetic patient's data (Table 1).

**Table 1** Distribution according to the cause of macrocrania.

| Cause of macrocrania | No | Sex |
|---|---|---|
| Group 1: Glutaric aciduria type 1 | 8 (40%) | 3 male, 5 female |
| Group 2: Benign macrocrania of infancy | 3 (15%) | 1 male, 2 female |
| Group 3: Van der Knapp | 3 (15%) | 3 female |
| Group 4: Mucopolysaccharidosis | 2 (10%) | 1 male, 1 female |
| Group 5: Canavan | 2 (10%) | 1 male, female |
| Group 6: Alexander | 1 (5%) | 1 male |
| Group 7: Gangliosidosis | 1 (5%) | 1 male |

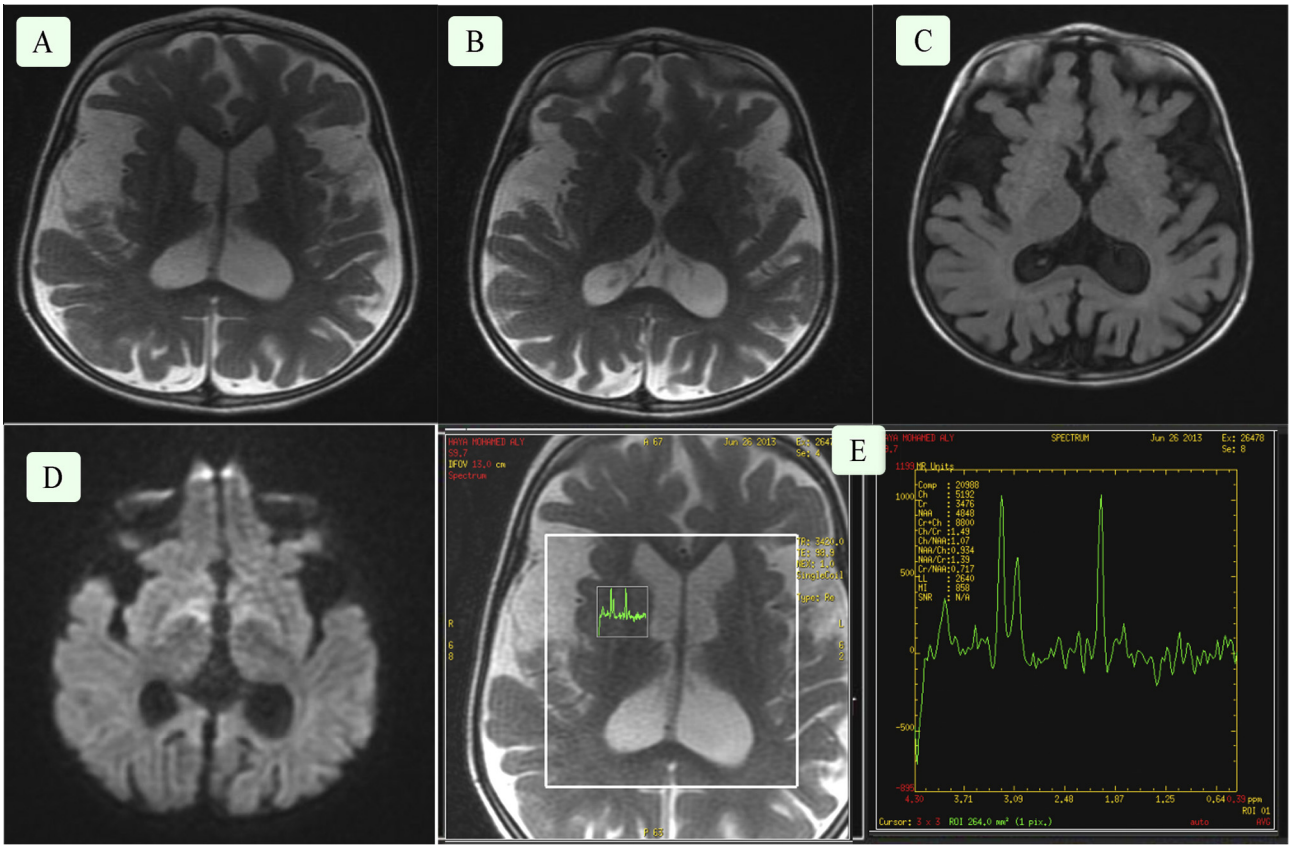


**Fig. 1** A 26 month old female child complaining of macrocrania and psychomotor regression. (A and B) Axial T2, (C) axial FLAIR, and (D) axial diffusion show moderate degree of atrophic changes of both cerebral hemispheres; however with special predilection of the fronto-temporal lobes bilaterally, this is associated with abnormally widened Sylvian fissures, abnormal bilateral symmetrical T2 and FLAIR hyperintense signal is seen involving the basal ganglia, yet sparing the thalami with mild diffusion restriction, still the white matter is normally myelinated for the patient's age and the corpus callosum is normal. The diagnosis was confirmed by MRS (E) of the abnormal deep gray matter showing elevated choline with preserved NAA peak, detectable lactate inverted doublet.

The study revealed a significant difference in the number of cases in each group within the abovementioned table and this was due to the limited duration of the study and the rarity of some disease.

### 3.1. Group 1: Glutaric aciduria type 1

This group included eight patients, their age ranged between 4 months and 22 months. They presented with macrocrania and variable clinical manifestations including GDD 50%, psycho-motor regression 50% and seizures 50%. One patient was in acute crisis showing hypotonia 12.5%. MRI findings included widened sylvian fissures in all patients (100%), the mesencephalic cistern was widened in 75%, and abnormal bilateral symmetrical T2 and FLAIR hyperintense signal involving the basal ganglia was in 87.5%. The diagnosis was confirmed by MRS in 4 patients showing elevated choline with preserved NAA, detectable lactate inverted doublet noted in one patient and by organic acid in urine in 4 patients. (Fig. 1)

### 3.2. Group 2: Benign macrocrania

This group included their age ranged between 14 and 18 months, they presented with macrocephaly with no other clinical manifestations, and they achieve normal developmental milestones. MRI findings included enlarged craniocortical, inter-hemispheric subarachnoid spaces beyond 5 mm and mildly dilated ventricles with normal brain myelination for age. The diagnosis was confirmed by MRS in one patient showing normal curve and ratios (Fig. 2).

### 3.3. Group 3: Van Der Knaap disease

This group included three patients, their age ranged between 10 months and 2 years, all were females (100%). They presented by macrocrania (100%), GDD 33.3%, psychomotor regression 66.6%, and seizures 66.6%. MRI findings showed bilateral symmetrical confluent white matter dysmyelination manifested as T1 hypo and T2 hyperintense signal affecting Centrum semiovale, corona radiata, external and extreme capsule, Periventricular white matter both anterior and posterior, The subcortical U fibers with bilateral frontotemporal subcortical cystic changes and subtle involvement of the cerebellar white matter was noted in one case (33.3%). The diagnosis was confirmed in 2 patients by MRS showing alternation between normal and reduced NAA within the affected white matter with no evidence of increased NAA in any of the affected areas. Choline peak also shows alternation between normal and increased peaks with resultant increase in Cho/NAA ratios (Fig. 3).

### 3.4. Group 4: Mucopolysaccharidosis

This group included two patients, their age were 17 month and 5 years, including one male and one female; they had

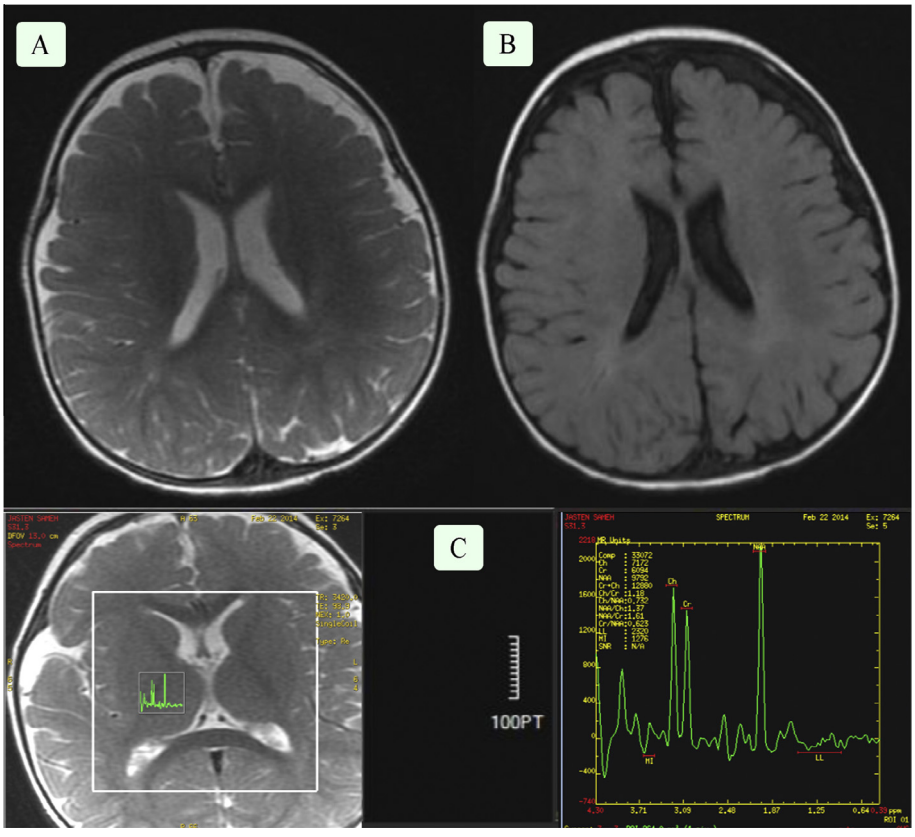


**Fig. 2** A 14 month old female child complaining of macrocrania with normal developmental milestones. (A) Axial T2 and axial FLAIR showed enlarged craniocortical, interhemispheric subarachnoid spaces beyond 5 mm, mildly dilated ventricles without gray matter or white matter signal changes. The diagnosis was confirmed by MRS (B) showing normal curves and ratios.

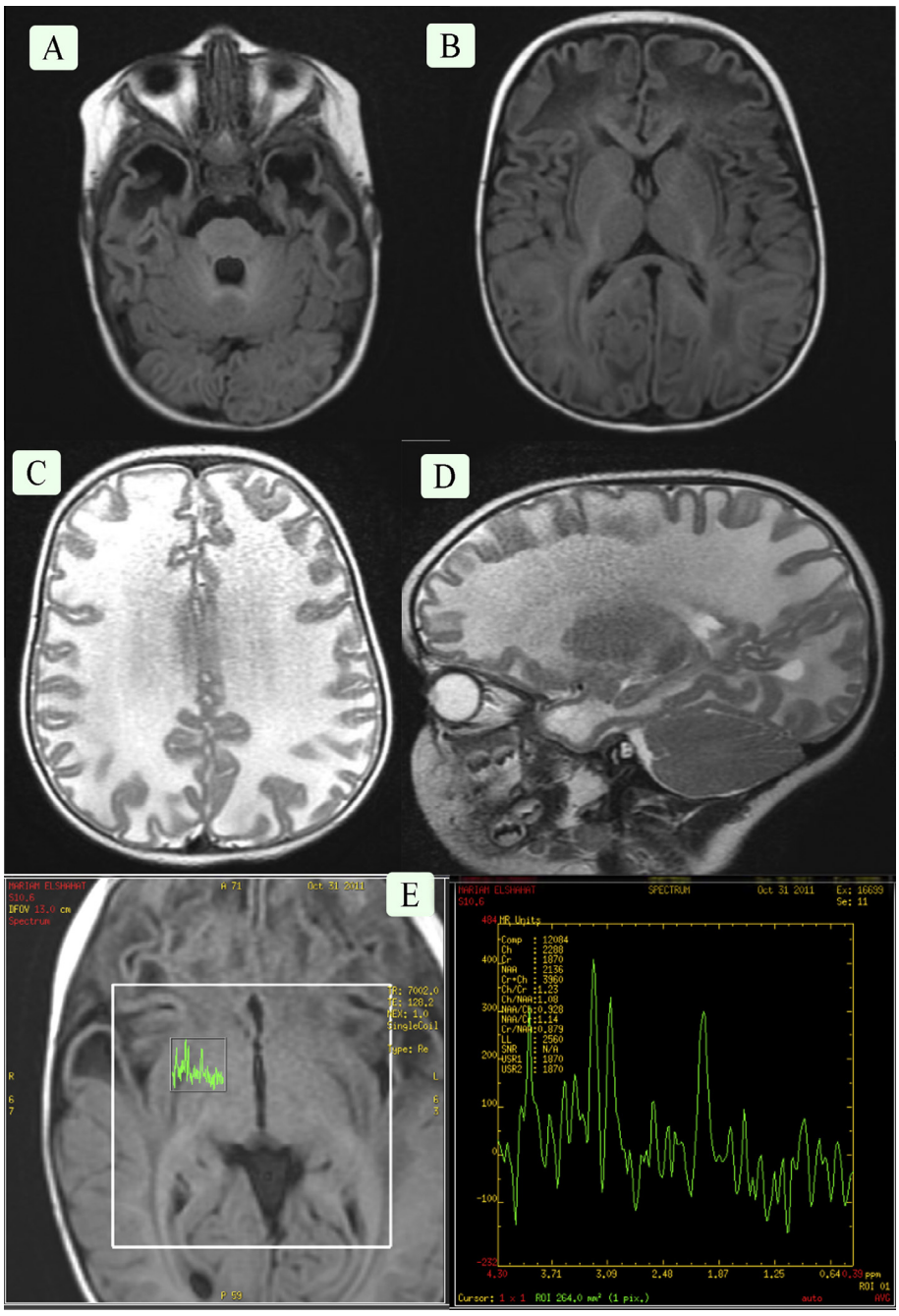


**Fig. 3** A 10 month old child complaining of macrocrania and global development delay. (A and B) Axial FLAIR, (C) axial T2WI, and (D) sagittal T2WI show bilateral symmetrical confluent white matter dysmyelination manifested as T1 hypo and T2 hyper-intense signal affecting Centrum semiovale, corona radiata, external and extreme capsule, Periventricular white matter both anterior and posterior, The subcortical U fibers Subtle involvement of the cerebellar white matter, sparing Corpus callosum as well as the internal capsule, and bilateral frontotemporal subcortical cystic changes. The diagnosis was confirmed by MRS (E) of the affected white matter showing alternation between normal and reduced NAA with no evidence of increased NAA in any of the affected areas. Choline peak also shows alternation between normal and increased peaks with resultant increase in Cho/NAA ratios.

characteristic coarse faces and flat nasal bridge. One patient had hepatosplenomegaly. The male patient presented with GDD, while the female patient showed progressive course of the disease manifested clinically as seizures hydrocephalus and joint contracture. The male patient shows early characteristic MRI findings of dilated Virchow Robin spaces noted mainly at the high frontal regions bilaterally.

The female patient showed in addition to the dilated Virchow Robin spaces progressive disease with characteristic MRI findings of hypoplasia of the corpus callosum, bifrontal

high convexity T1 hypo and T2 hyperintense subcortical white matter changes matching with demyelinating process, Macrocephaly with trigonocephalic configuration secondary to metopic beaking and generalized thickened calvarium. Narrowing of the foramen magnum with consequent compression on the cervicomedullary junction was also noted. The diagnosis was confirmed by MRS in one patient showing decreased NAA and increased choline/creatine ratio (Fig. 4).

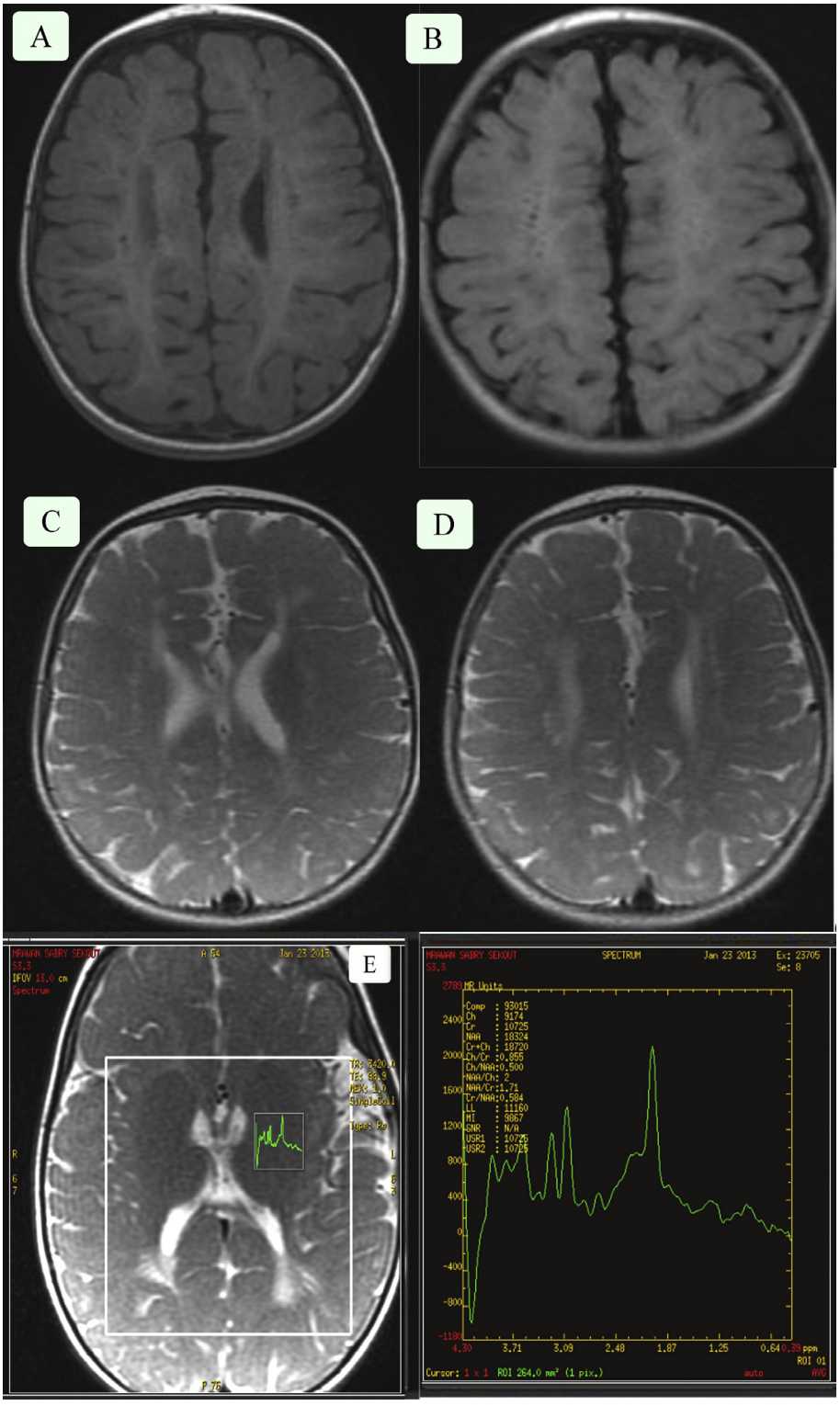


**Fig. 4** A 17 month old child complaining of macrocrania and global development delay. (A) Axial T1WI, (B) axial FLAIR, and (C and D) axial T2WI showed dilated Virchow Robin spaces mainly at the high frontal regions bilaterally, still no thickened calvarium or hypoplasia of corpus callosum. The diagnosis was confirmed by MRS (H) showing decreased NAA and preserved Ch/Creat ratio.

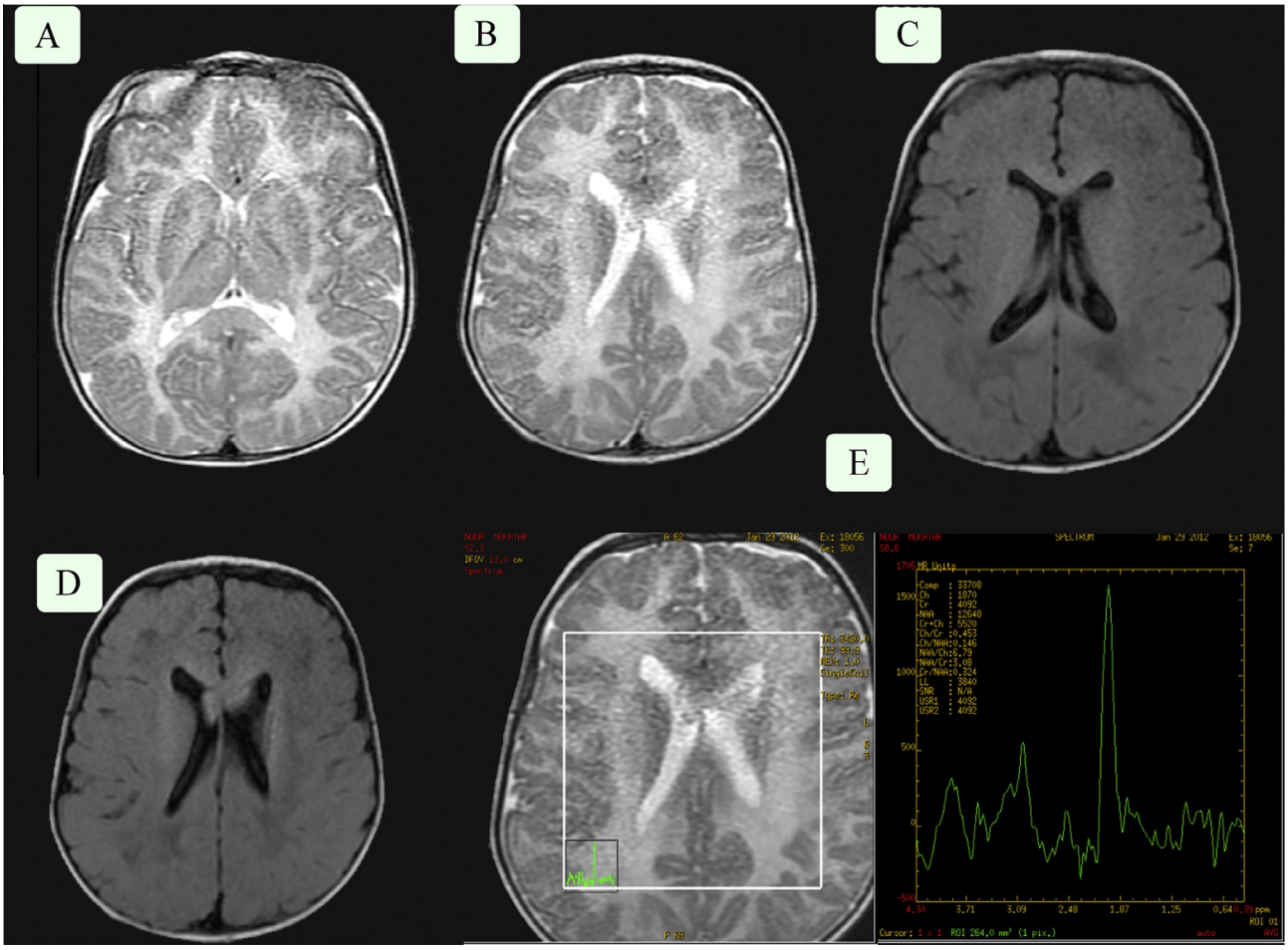


**Fig. 5** A 57 month old female child complaining of macrocrania, developmental delay and hypotonia. (A and B) Axial T2WI and (C and D) axial FLAIR show bilateral symmetrical extensive white matter dysmyelination involving nearly the entire tracts namely the periventricular, deep and subcortical U fibers, Still with preservation of the corpus callosum and internal capsules suggestive of centripetal progression pattern.

### *3.5. Group 5: Canavan disease*

This group included 2 patients with Canavan disease complaining of macrocrania, failure to achieve the expected developmental milestones and hypotonia. MRI findings included bilateral symmetrical extensive white matter dysmyelination noted as T2 hyperintensity and T1 hypointensity involving nearly the entire tracts namely the periventricular, deep and subcortical U fibers, still with preservation of the corpus callosum and internal capsules suggestive of centripetal progression pattern, and the deep gray matter was still intact. Both were confirmed by MRS of the affected white matter showing markedly elevated NAA with NAA/Ch ratio reaching 5 in one patient and 3.2 in the other patient (Fig. 5).

The diagnosis was confirmed by MRS (e) showing markedly elevated NAA with very high NAA/Ch ratio reaching 5 matching with infantile Canavan disease.

### *3.6. Group 6: Alexander disease*

This group included a 14 month old male presented with macrocrania and global developmental delay (floppy infant) and seizures showing 4 of the 5 characteristic MRI findings including (1) bilateral symmetrical confluent white matter abnormal myelination manifested as T2 and FLAIR hyperintense signal and hypointense in T1 sequence affecting the centrum semiovale, corona radiata, external and extreme capsule, periventricular white matter with anterior predilection, the subcortical U fibers still with sparing Corpus callosum as well as the internal capsule and the cerebellar white matter, (2) abnormal signal intensity in the basal ganglia, (3) a periventricular rim with high signal on T1-weighted images and low signal on T2-weighted images, and (4) postcontrast enhancement. The diagnosis was confirmed by MRS revealing increased NAA/Cr (see Fig. 6).

MRS showed increased NAA/Cr.

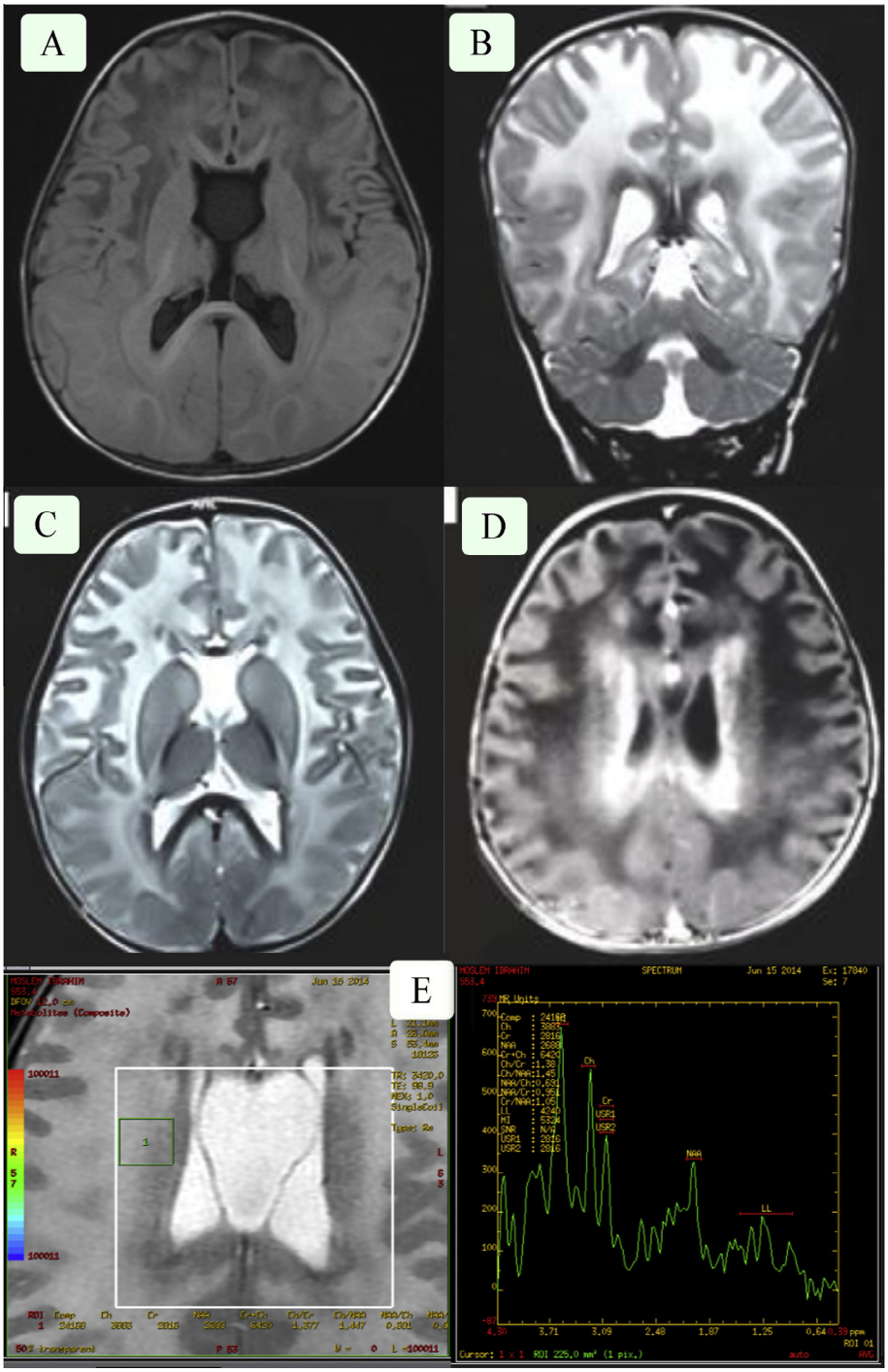


**Fig. 6** Case 6: A 14 month old child presented with macrocrania, developmental delay, and seizures. (A) Axial FLAIR, (B) coronal T2, (C) axial T2, (D) axial T1 postcontrast, and (E) MRS show bilateral symmetrical T2 hyperintensity with frontal predominance. Hyperintensity is also seen in the basal ganglia, intense enhancement of bifrontal periventricular WM, periventricular rim, and caudate heads. Less intense, patchy enhancement is seen in the putamen and thalami with less severe affection of the caudate and thalami.

### *3.7. Group 7: Gangliosidosis disease*

This group included a 17 month old male patient, presented with macrocrania and global developmental delay and seizures showing MRI findings of bilateral symmetrical T2 and FLAIR hyperintense putamen with less severe affection of caudate and thalami, also showed significant reduction in volume of the supratentorial white matter mainly the deeply seated WM at the level of corona radiata and centrum semiovale with consequent approximation of the corticoventricular distance, the corpus callosum and internal capsule were preserved bilaterally; also it showed mild degree of central atrophic changes

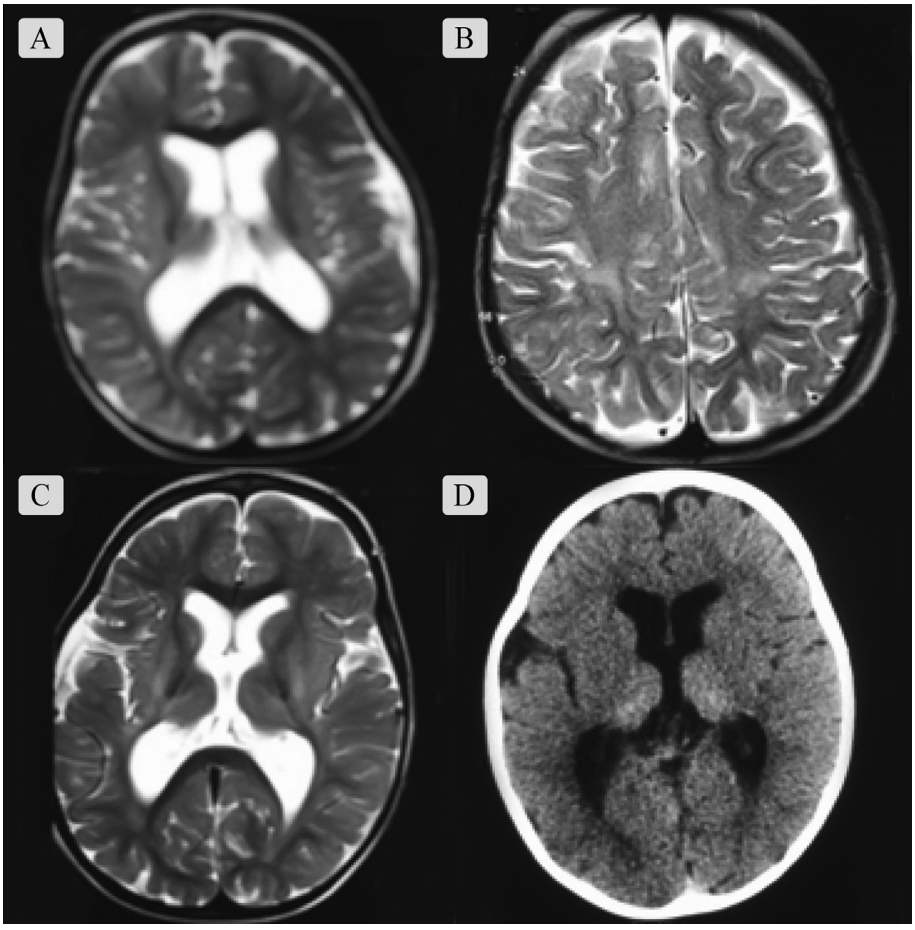


**Fig. 7** (A–C) Axial T2WI and (D) axial CT show bilateral symmetrical T2 and FLAIR hyperintense putamen with less severe affection of the caudate and thalami, this is associated with significant reduction in the volume of the supratentorial white matter mainly the deep seated white matter at the level of the corona radiata and Centrum semiovale with consequent approximation of the cortico-ventricular distance, still preserved corpus callosum and internal capsule bilaterally, mild degree of central atrophic changes is also noted in the form of supratentorial dilatation of the ventricular system, and CT shows bilateral symmetrical thalamic hyper-density.

manifested as supratentorial ventricular dilatation, and CT showed bilateral symmetric thalamic hyperdensities. The diagnosis was confirmed by fundus examination showing macular cherry red spot (see Diagram 2, Fig. 7 and Table 2).

## 4. Discussion

Head circumference measurement is an important physical examination to evaluate childhood growth and development because deviations from normal head growth patterns can indicate an underlying congenital, genetic, or acquired neurologic problem (1).

This study was carried out to demonstrate the different causes of non hydrocephalic macrocrania and the role of MRI to detect the different characteristic finding in each pathology.

The first group included eight patients diagnosed as glutaric aciduria type I, their age ranged between 4 months and 22 months. They presented with variable clinical manifestations including GDD 50%, psycho-motor regression 50%, and seizures 50%. One patient was in acute crisis showing hypotonia 12.5%.

Singh (10) described similar clinical manifestation in a 14-month-old boy who presented with loss of developmental milestones and tonic spasms following a diarrheal illness. He had mild motor delays, macrocephaly. He also reported the presence of axial hypotonia, and asymmetric dystonic posturing of neck and trunk.

On the other hand Hedlund et al. (11), suggested that the clinical manifestations of GA-1 can vary considerably even between siblings, suggesting an important environmental component. He reported that most patients have macrocephaly at birth or develop it shortly thereafter. Most of their patients have no clinical symptoms beyond a large head.

In our study we found characteristic MRI finding including widened sylvian fissures in all patients (100%), the mesencephalic cistern was widened in 75%, abnormal bilateral symmetrical T2 and FLAIR hyperintense signal involving the basal ganglia was in 87.5% which is consistent with the results of a study conducted by Twomey et al. (12) who found that widening of the sylvian fissures and of the fluid spaces anterior to the temporal lobes was seen in 93% of cases. The

**Table 2** Summary of the diagnostic findings in the 20 patients with macrocrania.

| Diagnosis | MRI finding | | | | MRS |
|---|---|---|---|---|---|
| | Characteristic feature | GM | WM | Others | |
| Glutaric aciduria ($n = 8$) | Wide operculum sign, abnormally widened Sylvian fissures | Bilateral symmetrical T2 and FLAIR hyperintense signal involving the basal ganglia, yet sparing the thalami with mild diffusion restriction | Peri-ventricular T2 and FLAIR hyperintense signal | Cerebellar atrophy is also noted manifested as widening of the cerebellar folia with consequent 4th ventricular ectasia | Elevated choline with preserved NAA peak. ± Detectable lactate inverted doublet |
| Benign macro-crania ($n = 3$) | Enlarged SAS beyond 5 mm | Normal GM myelination for age | Normal WM myelination for age | Mildly dilated ventricles | Normal curve and ratios |
| Van der Knapp ($n = 3$) | Bilateral frontotemporal subcortical cystic changes mainly evident on the FLAIR sequences | | Bilateral symmetrical WM changes manifested as T1 hypo and T2 hyperintensities affecting Centrum semiovale, corona radiata, external and extreme capsule, periventricular WM anterior and posterior and the subcortical U fibers, sparing the Corpus callosum and the internal capsule. +/- Involvement of the cerebellar WM | DWI: shows prominent hyposignal within the subcortical cysts and somewhat decreased signal within the affected white matter. The ADC is however increased | Alternation between normal and decreased NAA, Choline peak shows alternation between normal and increased peaks with resultant increase in Cho/NAA ratios |
| Canavan (n = 2) | | | Bilateral symmetrical extensive WM changes noted as T2 hyper and T1 hypointensity involving nearly the entire tracts still with preservation of the corpus callosum and internal capsules | | Markedly elevated NAA with very high NAA/Ch ratio |
| MPS ($n = 2$) | – Dilated Virchow Rubin spaces are noted bilaterally | | – Hypoplasia of the corpus callosum<br>– T1 hypo and T2 hyperintense subcortical WM changes | – Macrocephaly with trigonocephalic configuration<br>– thickened calvarium<br>– Narrowing of the foramen magnum with compression on the CM junction | Decreased NAA, increased Ch/Creatinine ratio; increased peak at 3.7 ppm |
| AD ($n = 1$) | | Abnormal signal of basal ganglia, thalami and brain stem | Bilateral symmetrical WM changes manifested as T2 /FLAIR hyperintense signal and hypointense in T1 with frontal predilection sparing Corpus callosum and the internal capsule | Intense enhancement Periventricular rim, frontal lobe WM, BG, thalami, BS (esp periaqueductal midbrain), dentate nuclei, fornix, optic chiasm | Increased NAA/Cr, increased myo-inositol/Cr, lactate doublet |
| GM 2 ($n = 1$) | | Bilateral symmetrical T2 and FLAIR hyperintense putamen with less severe affection of caudate and thalami | Reduction in volume of the supratentorial WM at the level of corona radiata and centrum semiovale with approximation of the corticoventricular distancePreserved corpus callosum and internal capsule bilaterally | Mild degree of central atrophic changes manifested as supratentorial ventricular dilatation | |

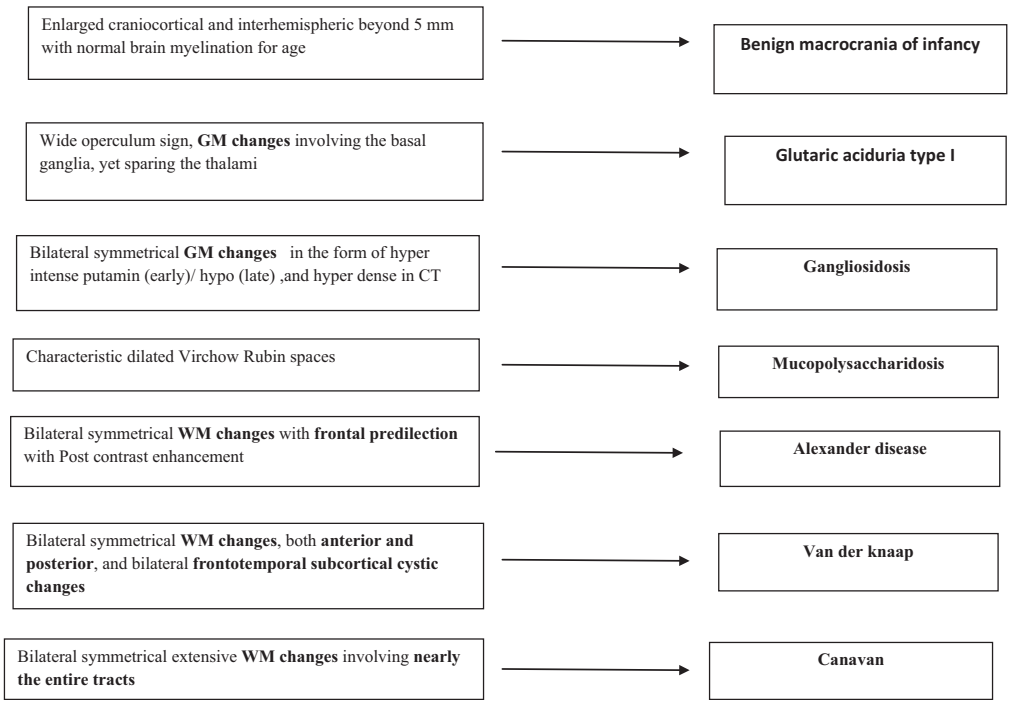


**Diagram 1** On the basis of these results, the key MRI findings for diagnosis of causes of macrocrania as a prominent clinical finding.

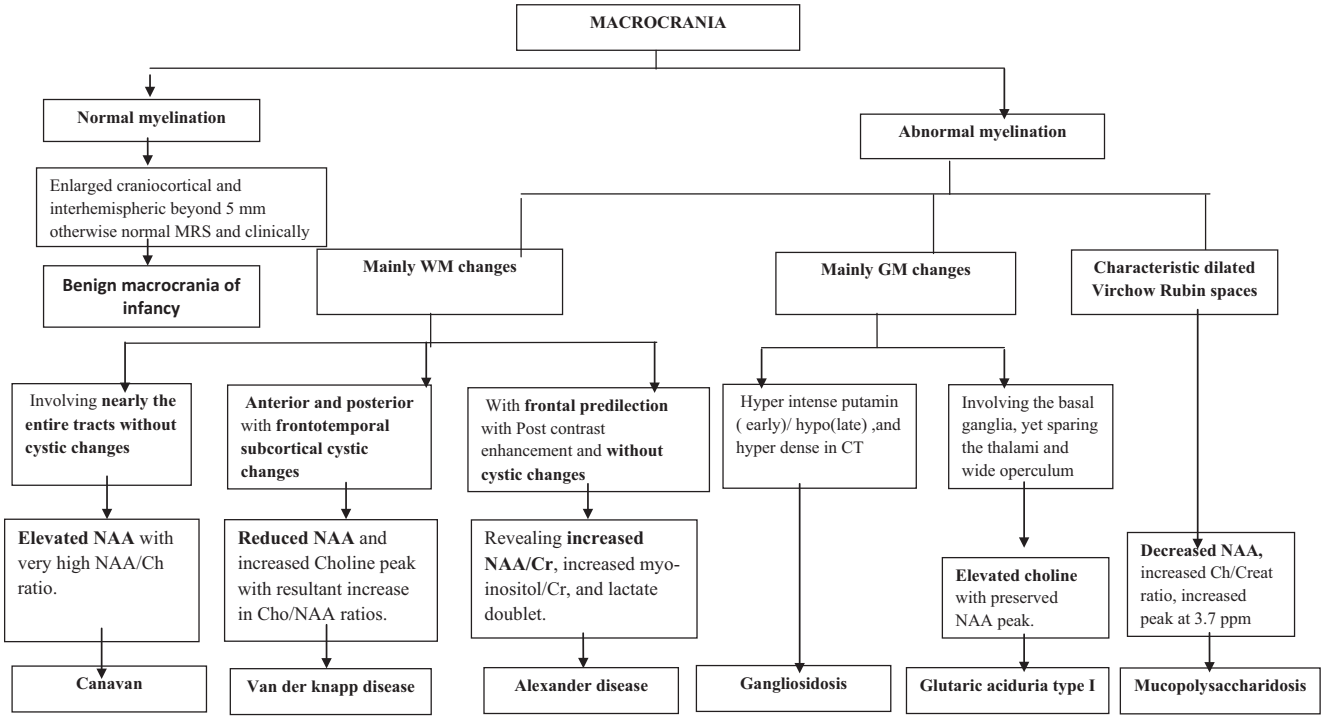


**Diagram 2** On the basis of these results, a flow chart was drafted for reviewing MRI scans for diagnosis of causes of macrocrania.

mesencephalic cistern was also widened in 86%. Abnormal high-signal intensity on T2-weighted (T2-W) images was seen in the basal ganglia and periventricular white matter in 64% of children (Fig. 1).

The subdural hygroma or subdural hemorrhage of glutaric acidemia type I was reported by Woelfle et al. (13) which may trigger an evaluation for child abuse. Hedlund et al. (11) suggested that subdural hygromas and subdural hemorrhages may

accompany cerebral atrophy. Cerebral atrophy, physiologic inertial cerebral forces, and tearing of bridging veins represent the most likely mechanism for the development of these collections. Alternatively, tears or fenestrations in the arachnoid membrane can lead to fluid accumulation within the subdural space. None of our cases showed subdural hygromas in their MRI.

Those MRI findings were also reported by various previous studies including Hedlund et al. (11), Singh et al. (10) and Martínez Granero et al. (14).

Four cases in our study were confirmed by MR Spectroscopy showing that the abnormal deep gray matter exhibits elevated Choline with preserved NAA peak while detectable lactate inverted doublet was noted in one patient.

Hedlund et al. (11) suggested that the presence of lactate particularly within the basal ganglia is an indirect index of impaired cerebral oxidative metabolism. Elevation of choline suggests cell membrane turnover which derives from neuronal loss and demyelination. The decline of N-acetylaspartate (NAA) reflects a combination of neuronal volume loss and neuronal dysfunction secondary to the presence of neurotoxic metabolic by-products.

On the other hand Bodamer et al. (15) reported that no consistent abnormalities in magnetic resonance spectroscopy have been identified in patients with glutaric acidemia type 1.

The second group included three patients diagnosed as benign macrocrania of infancy, their age ranged between 14 and 18 months, they presented with macrocephaly with no other clinical manifestations, and they achieve normal developmental milestones.

Alvarez et al. (16) found that about half of the studied 32 children were delayed in motor or language development at 5 months of age, but by 15–18 months of age all but one were found to be normal which is matching with our results.

On the other hand Muenchberger et al. (17) reported that out of their 15 patients, who were followed until adulthood, two had transient motor delay and two had speech delay at a mean age of 27 months.

Zahl et al. (6) suggested that it is difficult to define the limit between a normal and an enlarged subarachnoid space as the definitions used vary as does the subarachnoid space with age. However, a cranio-cortical width above 10 mm appears to be an absolute sign of pathology. The degree of ventricular dilatation is usually described as ''minimal'' or ''moderate'' without more specific measures: this probably explains the variation in incidence of patients with this finding.

Fukuyama et al. (18) were the first to describe tomographically the enlargement of the subarachnoid space in a study of 89 neurologically normal subjects, 43 of their children below the age of 10 years; they concluded that the visualization of the subarachnoid space in the frontal region beyond the age of 2 is always abnormal, while in the first and second years values above 8 mm and above 4 mm respectively were abnormal.

In our study, the cranio-cortical distance and the interhemispheric distance measure 5 mm and 6 mm respectively in the 14 month patients and 5 mm in the 14 month old patient (Fig. 2).

The third group included three patients diagnosed as van der knaap disease, and their age ranged between 10 months and 2 years presenting with macrocephaly 100% in addition to variable clinical presentations including GDD 33.3%, psychomotor regression 66.6%, and seizures 66.6% which is consistent with the results of Batla et al. (19) who reported 4 cases where macrocephaly was usually present at birth and after the first year. Seizures have been reported in half of the patients (49%) by Singhal et al. (20) and six of eight patients by Van der Knaap et al. (21). Significant disability due to motor as well as cognitive and language impairment was present in only one of their patients.

Batla et al. (19) suggested that the most important clue to the diagnosis is the radiological picture. The extensive white-matter changes in the brain with temporal subcortical cysts, sparing of the deeper structures have been considered the MRI hallmarks of the disorder. They also reported the presence of subcortical cysts in the anterior temporal region most commonly and often in the frontoparietal region which may increase in size and number over time, and the frontal involvement is variable and so is the cerebellar involvement which is consistent with our results where all patients (100%) showed bilateral frontotemporal subcortical cystic changes and subtle involvement of the cerebellar white matter was noted in one case (33.3%). (Fig. 3)

Also Batla et al. (19) reported the presence of posterior subcortical cysts as well in two of their patients.

Similar findings were also reported by various previous reports including Morita et al. (22) and Brockmann et al. (23).

The diagnosis was confirmed by MRS in two patients showing alternation between normal and reduced NAA. Choline peak also showed alternation between normal and increased peaks with resultant increase in Cho/NAA ratios which is consistent with the MRS finding reported by Morita et al. (22) of mildly reduced N-acetylaspartate (NAA).

Tu et al. (24) reported similar findings and suggested that NAA is believed to be of neuronal and axonal origin in mature brain, and its decrease is most likely due to axonal loss or dysfunction. They also suggested that low NAA may be the first sign of metabolic impairment in patients with VML, and that Choline increase is most likely due to enhanced myelin turnover related to demyelination and accumulation of membrane myelin degradation products.

Brockmann (23) reported marked reduction of N-acetylaspartate, creatine, and choline with normal values for myo-inositol, consistent with axonal loss and astrocytic proliferation.

The fourth group included two patients with mucopolysaccharidosis, and their age ranged between 17 months and 5 years, including one male and one female; they had characteristic coarse faces and flat nasal bridge. One patient had hepatosplenomegaly.

The first patient presented with GDD, while the second patient showed progressive course of the disease manifested clinically as seizures hydrocephalus and joint contracture.

The male patient shows early characteristic MRI findings of dilated Virchow Robin spaces noted mainly at the high frontal regions bilaterally (Fig. 4).

The female patient showed in addition to the dilated Virchow Robin spaces progressive disease with characteristic MRI findings of hypoplasia of the corpus callosum, bifrontal high convexity T1 hypo and T2 hyper-intense subcortical white matter changes matching with demyelinating process, Macrocephaly with trigonocephalic configuration secondary to metopic beaking and generalized thickened calvarium. Narrowing of the foramen magnum with consequent compression on the cervico-medullary junction was also noted.

Our findings were consistent with the results of a study conducted by Vedolin et al. (25) where all patients had a disease at onset below the age of 7 years. An exception could be MPS III patients.

Also our results were in agreement with the findings mentioned by Zafeiriou et al. (26) who demonstrated that signal-intensity abnormalities in the brain parenchyma represent a constant neuroimaging feature. Nevertheless, the frequency, magnitude, and time of occurrence of white matter abnormalities are variable in the different forms of MPS. The most commonly affected region is periventricular white matter. (25) Concerning deep gray matter signal-intensity abnormalities, changes have been described in the region of the basal ganglia (27).

This review also demonstrated that Communicating hydrocephalus is a well-recognized feature that occurs in most MPS types (25–28). It is usually only slowly progressive, with enlargement of subarachnoid and ventricular spaces representing its main neuroradiologic findings which is matching with our findings of communicating hydrocephalus in one patient.

On the other hand Shimoda-Matsubayashi et al. (28) described a unique imaging feature in the brain of patients with MPS is the "honeycomb-like" appearance in the basal ganglia and thalami in a 44-year-old patient with MPS II who exhibited patchy areas of increased and decreased signals in T1- and T2-weighted images in the above-mentioned brain regions. Apart from MPS II, this finding was also described in patients with MPS I and IIIB (26,28). None of our 2 patients showed this sign.

Manara et al. (29) recently showed that all patients with Hunter syndrome in their study had ventriculomegaly. Also they mentioned that cerebral atrophy represents one of the most prevalent MR imaging features in patients with MPS II and IIIB, (25) while it is also described in MPS I, IIIA, IIID, and VI (26) which is matching with our finding in the older patient.

Apart from cerebral atrophy, corpus callosum thinning was also described in patients with MPS I, II, IIIA, IIIB and VI (26) most probably as a result of ventricular dilation and enlarged PVS within this brain structure.

On the other hand patients with MPS have also been described as having abnormal MR imaging features concerning the area of the posterior cranial fossa. The most common among these findings is the presence of a mega cisterna magna, which is frequent in patients with MPS II (30) and has been also reported in MPS I and IIIB. (30) None of our patients shows these findings yet the older patient shows narrowing of the foramen magnum with consequent compression on the cervico-medullary junction which has been described by Manara et al. (31) and Zafeiriou (26) et al. in MPS II.

The most common craniocervical junction MR imaging features are spinal stenosis, compressive myelopathy, odontoid dysplasia, atlantoaxial instability, and dural thickening (26) which were not seen in our patients.

The diagnosis was confirmed by MRS in the younger patient showing decreased NAA and increased choline creatine ratio.

Takahashi et al. (31) also found an elevated Cho/Cr ratio in the WM of patients with MPS.

On the other hand Davison et al. (32) in a cohort of patients with MPS II reported that decreased N-acetylaspartate, total choline and glutamate in the white matter, and an elevation of myo-inositol were the main findings. Additionally, they have shown an alteration in N-acetylaspartate concentration during the disease progression, providing evidence that MR spectroscopy could be used as a monitoring tool demonstrating progressive neurologic impairment (32).

The fifth group included 2 patients with Canavan disease complaining of macrocrania, failure to achieve the expected developmental milestones and hypotonia.

They show characteristic MRI findings of bilateral symmetrical extensive white matter dysmyelination noted as T2 hyperintensity and T1 hypointensity involving nearly the entire tracts namely the periventricular, deep and subcortical U fibers, still with preservation of the corpus callosum and internal capsules suggestive of centripetal progression pattern, and the deep gray matter was still intact (Fig. 5).

Both were confirmed by MRS of the affected white matter showing markedly elevated NAA with NAA/Ch ratio reaching 5 in one patient and 3.2 in the other patient.

Our results were in agreement with the results of Hamidi et al. (33) who presented in a case report the clinical and specific imaging findings including MRI and MR spectroscopy revealed symmetric hyperintense signal changes extending to subcortical U fibers, globi pallidi, internal and external capsule, thalami and both dentate nuclei of cerebellum in their patient. Spectroscopy depicted markedly elevated NAA peak at the left Centrum semiovale. Increase in the NAA-to-choline ratio and the NAA to-creatinine ratio (2, 97 and 3, 79 respectively) were other significant findings suggestive of Canavan disease in their patient.

Also our results are consistent with the results described in a study conducted by Brismar et al. (34).

The sixth group included one patient diagnosed as Alexander disease.

According to a study by van der Knaap et al. (35), five MR imaging criteria were defined in Alexander disease: extensive cerebral white matter changes with frontal predominance, a periventricular rim with high signal on T1-weighted images and low signal on T2-weighted images, abnormalities of basal ganglia and thalami, brain stem abnormalities, and contrast enhancement of particular gray and white matter structures. Four of the five criteria had to be met for an MR imaging-based diagnosis.

In our study a 14 month old male presented with macrocrania and global developmental delay (floppy infant) and seizures showing 4 of the 5 characteristic MRI findings including (1) bilateral symmetrical confluent white matter abnormal myelination manifested as T2 and FLAIR hyperintense signal and hypointense in T1 sequence affecting the centrum semiovale, corona radiata, external and extreme capsule, periventricular white matter with anterior predilection, the subcortical U fibers still with sparing Corpus callosum as well as the internal capsule and the cerebellar white matter, (2) abnormal signal intensity in the basal ganglia, (3) a periventricular rim with high signal on T1-weighted images and low signal on T2-weighted images, and (4) postcontrast enhancement (Fig. 6).

Our results were in agreement with most of the previous studies including Dinopoulos et al. (36) and Gingold et al. (37).

On the other hand Dinopoulos et al. (36) reported brain stem lesions in eight of the 10 patients. Most frequently affected were the midbrain (in the anterior part, the periaqueductal region, or the entire area except for the red nuclei and

colliculi) and the medulla (either in the posterior or in the central part). The pontine tegmentum was affected in some patients. In our patient no brain stem lesions were detected.

Our results were confirmed by characteristic MRS showing increased NAA/Cr, increased myo-inositol/Cr, and presence of lactate doublet which were in agreement with the results of MR spectroscopy by Dinopoulos et al. (36) acquired within the frontal white matter demonstrating abnormally low levels of N-acetylaspartate (NAA), high levels of myo-inositol (mIns), and lactic acid.

The seventh group included a 17 month old male patient, presented with macrocrania and global developmental delay and seizures showing characteristic MRI findings of bilateral symmetrical T2 and FLAIR hyperintense putamen with less severe affection of caudate and thalami, and showed significant reduction in volume of the supratentorial white matter mainly the deeply seated WM at the level of corona radiata and centrum semiovale with consequent approximation of the corticoventricular distance, the corpus callosum and internal capsule were preserved bilaterally; also it showed mild degree of central atrophic changes manifested as supratentorial ventricular dilatation and CT showed bilateral symmetric thalamic hyperdensities.

Our results were in agreement with most previous studies including Steenweg et al. (38) and Grosso et al. (39) showing characteristic MRI features as mild T2 hyperintensity of the caudate nucleus and putamen with signs of diffuse hypomyelination, contrasting with a normal T2 signal intensity of the corpus callosum, indicating more complete myelination of this structure. The anterolateral part of the thalamus was slightly abnormal in signal in a few patients.

Maegawa et al. (40) reported 21 new cases and reviewed 134 previously reported patients with GM2 gangliosidosis. In their series, the most frequent finding was cerebellar atrophy that was followed by generalized cerebral atrophy. Interestingly, 17.1% of the patients had normal neuroimaging studies.

On the other hand Bano et al. (41) demonstrate in a case report that in both the Tay-Sachs (variants B and B1) and Sandhoff diseases, the thalami demonstrate symmetrical hyperdensity on CT, and hyper/hypo-signal intensity on T1/T2-weighted MR images, respectively. These density/intensity changes in the thalami and mesial temporal lobe gyri probably reflect the accumulation of calcium and GM2 ganglioside. Mid brain and corpus callosum atrophy in these patients has invariably seen attributed to disturbed myelination and Grosso et al. (39) and Beck et al. (42).

## 5. Conclusion

Conventional MRI is helpful and is of great value in the early detection and diagnosis of different causes of non hydrocephalic macrocrania.

MRS is helpful in differentiating between benign macrocrania of infancy from other dysmyelinating diseases and was specific in Canavan disease.

## Conflict of interest

We have no Conflict of interest.

## References


(1) Medina LS, Frawley K, Zurakowski D, Buttros D, DeGrauw AJC, Crone KR. Children with macrocrania: clinical and imaging predictors of disorders requiring surgery. AJNR 2001;22:564–70.
(2) Jeong G, Kim M, Han BH. Clinical features of macrocephaly at birth in Korea. Korean J Pediatr 2014;57(2):75–8.
(3) Rutherford M, Counsell S, Allsop J, Boardman J, Kapellou Olga, David Larkman, et al. MRI of the neonatal brain part 2 chapter 4 Frances M Cowan. Magnetic resonance imaging of the normal infant brain: term to 2 years. Pediatrics 2004;114:1004–14.
(4) Alexandra T, Vertinsky, Patrick D, Barnes. Macrocephaly, increased intracranial pressure, and hydrocephalus in the infant and young child. Top Magn Reson Imaging 2007;18:1.
(5) Emily B, Ridgway, Howard L, Weiner. Skull deformities. Pediatr Clin N Am 2004;51:359–87.
(6) Zahl SM, Egge A, Helseth E, Wester K. Benign external hydrocephalus: a review, with emphasis on management. Neurosurg Rev 2011;34:417–32.
(7) Kumar R. External hydrocephalus in small children. Childs Nerv Syst 2006;22:1237–41.
(8) Delmonaco AG, Gaidolfi E, Scheper GC, Girardo E, Molinatto C, Belligni E, et al. A child with macrocephaly: case report of a patient with megalencephalic leukoencephalopathy with subcortical cysts and a compound heterozygosity for two mutations in the MLC1 gene. Minerva Pediatr 2011 Apr;63(2):125–9.
(9) Kaiser GL. Symptoms and signs in pediatric surgery. Berlin Heidelberg: Springer-Verlag; 2012, ISBN978-3-642-31161-1(e-Book).
(10) Singh P, Goraya JS, Ahluwalia A, Saggar K. Teaching neuroimages: glutaric aciduria type 1 (glutaryl-CoA dehydrogenase deficiency). Neurology 2011;77:e6. http://dx.doi.org/10.1212/WNL.0b013e31822313f6.
(11) Hedlund GL, Longo N, Pasquali M. Glutaric Acidemia Type 1. Am J Med Genet C Semin Med Genet 2006 May 15;142C(2):86–94.
(12) Twomey EL, Naughten ER, Donoghue VB, Ryan S. Neuroimaging findings in glutaric aciduria type 1. pediatr Radiol 2003;33(12):823–30.
(13) Woelfle J, Kreft B, Emons D, Haverkamp F. Subdural hemorrhage as an initial sign of glutaric aciduria type 1: a diagnostic pitfall. Pediatr Radiol 1996;26:779–81.
(14) Martínez Granero MA, Garcia Pérez A, Martínez-Pardo M, Parra E. Macrocephaly the first manifestation of glutaric aciduria type I: the importance of early diagnosis. Neurologia 2005;20(5):255–60.
(15) Bodamer OA, Gruber S, Stockler-Ipsiroglu S. Nuclear magnetic resonance spectroscopy in glutaryl-CoA dehydrogenase deficiency. J Inherit Metab Dis 2004;27:877–83.
(16) Alvarez LA, Maytal J, Shinnar S. Idiopathic external hydrocephalus: natural history and relationship to benign familial macrocrania. Pediatrics 1986;77:901–7.
(17) Muenchberger H, Assaad N, Joy P, Brunsdon R, Shores EA. Idiopathic macrocephaly in the infant: long-term neurological and neuropsychological outcome. Childs Nerv Syst 2006;22:1242–8.
(18) Fukuyama Y, Miyao M, Ishizu T, Maruyama H. Developmental changes in normal cranial measurements by computed tomography. Dev Med Child Neurol 1979;21:425–32.
(19) Batla A, Pandey S, Nehru R. Megalencephalic leukoencephalopathy with subcortical cysts: a report of four cases. J Pediatr Neurosci 2011;6(1):74–7.
(20) Singhal BS, Gorospe JR, Naidu S. Megalencephalic leukoencephalopathy with subcortical cysts. J Child Neurol 2003;18:646–52.
(21) Van der Knaap MS, Barth PG, Stroink H. Leukoencephalopathy with swelling and a discrepantly mild clinical course in eight children. Ann Neurol 1995;37:324–34.

(22) Morita H, Imamura A, Matsuo N, Tatebayashi K, Tatebayashi K, Kentaro Omoya, et al. MR imaging and 1H-MR spectroscopy of a case of van der Knaap disease. Brain Dev 2006;28(7):466–9.
(23) Brockmann K, Finsterbusch J, Terwey B, Frahm J. Megalencephalic leukoencephalopathy with subcortical cysts in an adult: quantitative proton MR spectroscopy and diffusion tensor MRI. Neuroradiol 2003;45(3):137–42.
(24) Tu YF, Chen CY, Huangb CC, Lee CS. Vacuolating megalencephalic leukoencephalopathy with mild clinical course validated by diffusion tensor imaging and MR spectroscopy. AJNR 2004;25:1041–5.
(25) Vedolin L, Schwartz IV, Komlos M, et al. Correlation of MR imaging and MR spectroscopy findings with cognitive impairment in mucopolysaccharidosis II. AJNR Am J Neuroradiol 2007;28:1029–33.
(26) Zafeiriou DI, Batzios SP. Brain and spinal MR imaging findings in mucopolysaccharidoses: a review. AJNR 2013;34:5–13.
(27) Taccone A, Tortori Donati P, Marzoli A, Dell'Acqua A, Gatti R, Leone D. Mucopolysaccharidosis: thickening of dura mater at the cranio-cervical junction and other CT/MRI findings. Pediatr Radiol 1993;23:349–52.
(28) Shimoda-Matsubayashi S, Kuru Y, Sumie H, Ito T, Hattori N, Okuma Y, et al. MRI findings in the mild type of mucopolysaccharidosis II (Hunter's syndrome). Neuroradiol 1990;32:328–30.
(29) Manara R, Priante E, Grimaldi M, Lucia Santoro, Luca Astarita, Rita Barone, et al. Brain and spine MRI features of Hunter disease: frequency, natural evolution and response to therapy. J Inherit Metab Dis 2011;34:763–80.
(30) Seto T, Kono K, Morimoto K, Inoue Y, Shintaku H, Hattori H, et al. Brain magnetic resonance imaging in 23 patients with mucopolysaccharidoses and the effect of bone marrow transplantation. Ann Neurol 2001;50:79–92.
(31) Takahashi Y, Sukegawa K, Aoki M, et al. Evaluation of accumulated mucopolysaccharides in the brain of patients with mucopolysaccharidoses by (1)H-magnetic resonance spectroscopy before and after bone marrow transplantation. Pediatr Res 2001;49:349–55.
(32) Davison JE, Hendriksz CJ, Sun Y, et al. Quantitative in vivo brain magnetic resonance spectroscopic monitoring of neurological involvement in mucopolysaccharidosis type II (Hunter Syndrome). J Inherit Metab Dis 2010 [Epub ahead of print].
(33) Hamidi C, Aydin E, Goya C, et al. Finding Canavan disease, and diagnostic hallmark MR-spectroscopy. IJBCS 2012;1(II):75–9.
(34) Brismar J, Brismar G, Gascon G. Canavan disease: CT and MR imaging of the brain. Am J Neuroradiol 1990 [PubMed – indexed for MEDLINE].
(35) van der Knaap MarjoS, Naidu Sakkubai, et al. Alexander disease: diagnosis with MR imaging. AJNR Am J Neuroradiol March 2001;22:541–52.
(36) Dinopoulos A, Gorospe JR, Egelhoff JC. Discrepancy between neuroimaging findings and clinical phenotype in Alexander disease. AJNR Am J Neuroradiol 2006;27:2088–92.
(37) Gingold MK, Bodensteiner JB, Schochet SS, Jaynes M. Alexander's disease: unique presentation. J Child Neurol 1999;14:325–9.
(38) Steenweg M.E., Vanderver A, Blaser S et al. Magnetic resonance imaging pattern recognition in hypomyelinating disorders. 2971–2982 First published online; 29 September 2010.
(39) Grosso S1, Farnetani MA, Berardi R, et al. GM2 gangliosidosis variant B1 neuroradiological findings. J Neurol 2003;250 (1):17–21.
(40) Maegawa GH, Stockley T, Tropak M, et al. The natural history of juvenile or subacute GM2 gangliosidosis: 21 new cases and literature review of 134 previously reported. Pediatrics 2006;118:1550–62.
(41) Bano S, Prasad A, Yadav S N, et al. Neuroradiological findings in GM2 gangliosidosis variant B1. J Pediatr Neurosci 2011;6 (2):110–3.
(42) Beck M, Sieber N. GoebelHH. Progressive cerebellar ataxia in juvenile GM2 gangliosidosis type Sandhoff. Eur J Pediatr 1998;157:866–7.